PAPER • OPEN ACCESS

Performance of homogeneous charge compression ignition (HCCI) engine with common rail fuel injection

View the article online for updates and enhancements.

Performance of homogeneous charge compression ignition (HCCI) engine with common rail fuel injection

W Niklawy[1], M Shahin[2], M I Amin[3] and A Elmaihy[3]
[1] PhD candidate, Mechanical Power Engineering Department, Military Technical College, Cairo, Egypt.
[2] Mechanical Engineering Department, School of Engineering, Badr University, Badar, Cairo, Egypt.
[3] Mechanical Power Engineering Department, Military Technical College, Cairo, Egypt

niklawywaleed@gmail.com

Abstract. Homogeneous Charge Compression Ignition (HCCI) engine is a newly introduced technology. However, controlling the HCCI timing of ignition and theheat release rate, at all operating regimes, present the biggest challenge due to the complicated and highly coupled combustion problems. The successful implementation of the common rail injection system in diesel engines has made this possible. The main key for this success is the capability to optimize the most important fuel injection parameters, namely timing, rate, and duration.This work experimentally investigates the performance of an HCCI Diesel engine with a Common Rail Direct Injection (DI) fuel system. The engine used is a turbocharged 2776 cc, 4-stroke, 4-cylinder, water-cooled with overhead valve mechanism. The engine performance is evaluated and presented at different loads and speeds. The Apparent Heat Release Rate during combustion is evaluated from the measured cylinder pressure-crank angle data. The pressure in the fuel line is measured at the entry to different fuel injectors to investigate the effect of pressure wave propagation in the fuel line on the fuel injection system.

1. Introduction
Although diesel engines have high thermal efficiencies than that for petrol engines, they release higher amounts of NOx, smoke and particulate matter (PM). To defeat these drawbacks, a relatively new combustion concept known as HCCI (Homogeneous charge compression ignition) is being explored all overt he world. HCCI engines can operate with reduced NOx, smoke and PM emissions simultaneously [1-3].HCCI was developed as a consequence of current progress in electronic engine control, variable valve timing and lift systems, so the implementation of the HCCI combustion concept in the manufacture of engines is now considered to be practical [4,5].HCC uses the advantages of spark ignition and compression ignition engines. They have better thermal efficiency than that for Spark Ignition engines and come up with the efficiency of a Compression Ignition engine [6-7].

Homogeneous Charge Compression Ignition (HCCI) uses a lean homogeneous air-fuel mixture as a means to decrease the combustion temperature. This mixture can be carried out by prolonging the ignition delay period with extremely advanced injection timing. Most of the fuel is injected, evaporated and mixed in the premixed mode of combustion, such that the mixture at the moment of

ignition is near homogeneous. Therefore, the premixed mode of combustion is the predominant phase in HCCI [8]

In recent times, the multiple injection approach was useful in commercial common rail Direct Injection HCCI diesel engines to accomplish an organized air-fuel mixture and evade wall wetting. The common rail system provides higher injection pressure for better fuel spray atomization and evaporation, improved air entrainment and mixing in the fuel jet, which is advantageous for lowering soot emissions [9,10]. Several Direct Injection HCCI concepts have used advanced injection circumstances to sufficiently prolong the ignition delay period so that full fuel vaporization event preceding to combustion. The electronically controlled common rail injection permits diesel engines to vary the injection timing broadly and also gives the ability to achieve multi- injection strategies which result in improved charge mixing and homogeneity [11].

During HCCI engine running, a homogeneous fuel and air mixture is set throughout the compression process and the mixture auto ignition takes place by compression only at different in-cylinder positions when reaching the chemical activation energy. The combustion process is controlled entirely by chemical kinetics like Compression ignition engines [12] instead of ignition by a spark followed by a flame front propagation such as Spark Ignition engine [13]. The two-step heat release processes with low-temperature kinetic (cool) reactions occurring firstly followed by high-temperature kinetic reactions are noticed in HCCI engine combustion.

Many researchers have studied the effect of engine speed on the combustion behavior and performance characteristics of a HCCI engine. Kong et al. [14] investigated the consequence variations of ignition startmoment on HCCI engine combustion at different speeds. They concluded that the ignition start would be an efficient and practical required parameter to manage timing of ignition for the dynamic engine regimes. Iida et al. [15] concluded that the start of heat release is less sensitive to engine speed variations than that of compression ratio, suction air, and coolant water temperatures. Aroonsr isopon et al. [16] experimentally examined different reference fuels with an octane number of 70, which reveal significant heat release at low-temperature, at different engine speeds from 600 to 2000 rpm with constant suction air temperature. It was found that the low-temperature heat release period decreases as engine speed increases. Furthermore, decreasing low-temperature heat release duration causes shifting the high-temperature heat release period to later timings, consequently, a long low-temperature (cool) heat release period resulted in maintain high-temperature heat release. Iida et al. [17] used n-butane as a fuel to investigate the effect of inlet air temperature, compression ratio and engine speed on HCCI operating ranges in a research engine. they found that operation of HCCI at a relatively high engine speed was achieved of 2000 rpm, with a high compression ratio and a high temperature inlet air of 16.55 and 400 K, respectively. Szybist and Bunting [18] concluded that the amount of energy released during the low-temperature heat release interval increased suddenly as engine speed reduced. Besides, a nearly constant temperature rise which occurred during the low-temperature heat release period was noticed for all engine operating conditions. Garcia et al. [19] and Genzale et al. [20] reported that the angle of the start of combustion increases as the engine speed increases. Agarwal [21] concluded that the maximum pressure rise rate and coefficient of indicated mean effective pressure[IMEP] variation are the critical factors, that can be used to characterize HCCI operating range. Ebrahimi and Desmet [22] experimentally studied the effect of engine speed and cyclic variations in an HCCI engine.

Khandal et al [5] presented an exhaustive review on the performance characteristics, exhaust emission and combustion behavior of Common Rail Direct Injection and HCCI engines operated using with different fuels. Hadia et al [23] numerically investigated the combined effects on efficiency of the compression ratios and steam injection, characteristics of combustion and emissions of an HCCI engine. The contaminant emission is restricted by the dilution of the reactant by using steam injection. Combustion is performed by using engine modeling.

Calam et al [24] parametrically investigated the effects of compression ratio on HCCI combustion, performance, and emissions. The engine operational BSFC maps were the results of running the

engine at 169 experimental data points. The experiments were carried out at different equivalence ratios with predetermined intake air temperature (353 K) and by using RON20 and RON40 fuels.

El Shenawy et al [25] reported that one of the essential aspects to reduce engine emissions is how to prepare a homogenous charge for HCCI engines. One strategy is the external mixture formation, or port fuel injection (PFI). PFI used only for high volatile fuel such as alcohol [26-28].

The second is the in-cylinder mixture preparation, which can be classified according to injection timing early injection in which fuel is injected in the compression stroke and late injection. in which fuel injection is delayed behind the top dead center [29].

One of the main challenges that the HCCI combustion technique has to face is the occurrence of knocking at high loads due to high combustion pressure which causes the engine to knock. This may limit this technique commercially practical [30]. However, there are very few studies investigating the effects of the external load on HCCI engines parametrically at different engine speeds. The objective of this work experimentally investigates the performance of an HCCI Diesel engine with a Common Rail Direct Injection (DI) fuel system. The engine performance is evaluated and presented at different loads and speeds. The Apparent Heat Release Rate during combustion is evaluated from the measured cylinder pressure-crank angle data. The pressure in the fuel line is measured at the entry to different fuel injectors to investigate the effect of pressure wave propagation on the fuel line pressure at different operating conditions.

2.The Test Facility (Experimental Setup)

Experimental investigations were implemented on a transport diesel engine of type Mercedes-Benz with an open chamber. A four in-line cylinders, water-cooled direct injection diesel engine with over-head valve gear and "common rail" fuel injection system. (available in the laboratory of mechanical power and energy at the Military technical college) The main engine design parameters are listed in table 1. The test rig includes the engine and all the instrumentation necessary for measuring and recording the operating parameters. An on-line data acquisition system is furnished to improve the speed and accuracy of data collection and recording. is used. Detailed engine data are given in table 1.

Table 1. Engine data.

Description	Specification
Engine	R2816K5A
Bore	94 mm
Stroke	100 mm
weight	270 kg
Compression Ratio	17.5
Number of Cylinders	4
Displacement	2776 cc
Max power	90 kW (120H.P.) @ 3800 RPM
Peak Torque	400 N·m @ 1800 RPM
Fuel primary pump	Electric pump
Fuel System	Direct Fuel Injection Common Rail
High-Pressure Fuel	Radial Piston Pump (3 pistons)
Injection pump	CP3 2nd Generation Common Rail
Timing System	Valve Belt Driven DOHC Overhead

2.1 Instrumentations

The parameters measured are classified into three main groups. a -External parameters: Engine speed, engine load, fuel consumption, airflow, crank angle, ambient conditions and real-time. B-Internal parameters: pressure inside the cylinder, inlet and exhaust manifolds and fuel line,and turbocharger speed. C-Safety parameters: Lubricating oil pressure and temperature, and cooling water, temperature. Figure 1 gives a general scheme of installed test rig showing numbered locations where important

pickups and transducers are positioned. A list of these locations and the corresponding measured parameter used in this study at each is given below is given in table 2.

Engine external loading was carried out by an ELZE /Heenan hydraulic dynamometer. The fluid used was water with which the maximum braking power could reach 170 kW at 4000 rpm. The engine and dynamometer shafts were directly coupled through a cardan shaft. An S-type load cell (strain gauge S type, max capacity 500kg) is inserted under the dynamometer torque reaction arm. The load cell is completed with a bridge amplifier that is excited (12VDC) from a regulated power supply. The whole setup is calibrated by applying known weights on the cell and observing the net voltage output.

A water-cooled piezoelectric transducer (type PCB model no. 112B11) is used for measuring cylinder pressure. The charge amplifier used is a PCB type, with the capability of statically holding the output charge for calibration processes. The transducer is mounted on the cylinder head above cylinder no.1 where suitable and enough space could be provided. The glow plug of this cylinder was machined from the inside to form a cavity. The sensor is mounted at the outer side of the cavity that is opened to the combustion chamber on the inner side

A piezoelectric transducer type (Kistler PN 6278) and charge amplifier type (Kistler SN 284625) is used to measure fuel line pressure. This setup is capable of measuring pressure up to 3000 bars. The transducer is directly mounted on the fuel line high pressure connecting the rail to an injector no.1. The transducer, amplifier, and cabling were calibrated together using the deadweight tester
Engine fuel consumption at steady-state operation is evaluated by recording the time of consumption of a certain volume of fuel. This old method remains particularly valuable today because of the high accuracy achieved. The measuring device consists of a glass flask of 250 cc volumes, an auxiliary fuel tank, a control cock, and a stopwatch.
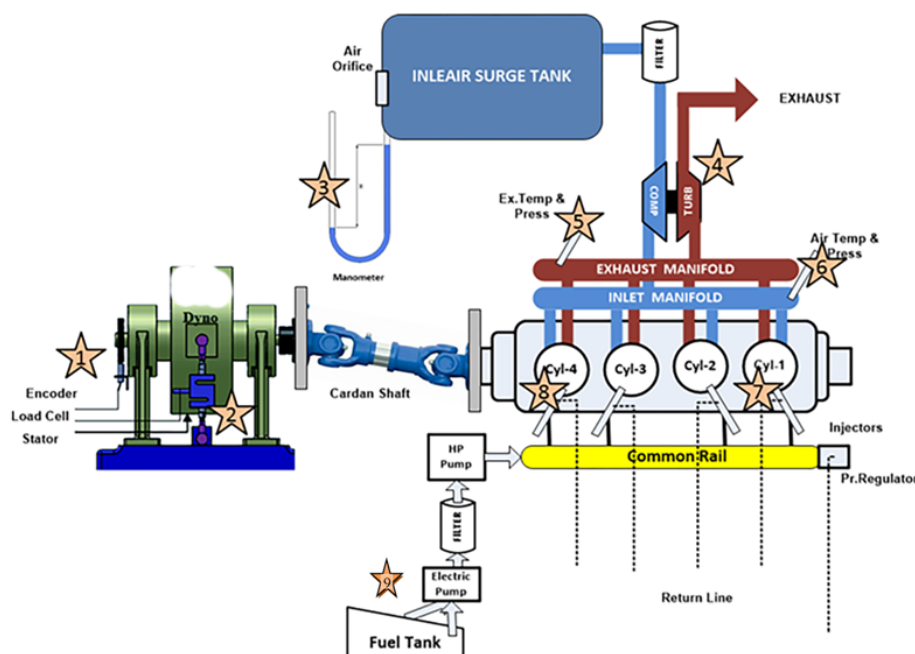
Figure 1. Scheme of the engine test facility.

An incremental digital quadrature encoder (type WDG 58B-360-ABN-G24-K3) is used for engine speed measurement. The encoder gives 2 trains of pulses (A and B), each has 360 pulses per encoder shaft revolution. The two trains are phased by ¼ pulse, and a third index train (N) with one pulse per each revolution is also produced. The Encoder is mounted on a special bracket fixed at the free end of the dynamometer shaft, figure 1.

A standard orifice (40 mm) diameter is mounted at the air surge tank entrance with a U-tube water manometer for measuring the air pressure drop across the orifice. The airflow rate is calculated from the orifice area and the manometer reading. This technique is considered as one of the most accurate methods for measuring the fluid flow rate.

The unsteady pressure in the exhaust manifold is measured using a strain gauge transducer (model PT124BG1/4) which comes complete with its amplifier). The transducer is positioned such as direct exposure to the exhaust blows from cylinder outlet ports are avoided.

Table 2.A list of measured parameters and the corresponding locations relevant to figure 1.

Location	Measured Parameters	Instrument	Accuracy
1	Engine Speed & Crank Angle	Incremental Encoder (WD GI 58B)	+ 7.5 % of the pulse width
2	External load (Torque)	S-type load cell	Combined error $\leq$+0.05%
3	Inlet air pressure drop across the orifice pressure	U tube manometer	NA
5	Exhaust Temperature	Thermocouple type K (Nicr-Ni)	+/- 2.2C or +/- .75%
	Exhaust Pressure	Strain gauge transducer model PT124BG1/4	0.5%FS, 1.0%FS
6	Inlet Air Temp	type K (Nicr-Ni)	+/- 2.2C or +/- .75%
	Inlet Air Pressure	strain gauge transducer model AST4000AV0015P6C0000	$\leq\pm$ 0.5% BFSL
7	Cylinder pressure	piezoelectric transducer type PCB (model no. 112B11)	<2.0 % FS
8	Fuel pressure sensor	piezoelectric transducer type (Kistler PN 6278)	<0.2 % FS
9	Fuel Consumption	Calibrated Bowel	NA

A strain gauge pressure transducer (model AST4000AV0015P6C0000, complete with an amplifier, is used for measuring the pressure inside the intake manifold. Thermocouples type K (Nicr-Ni), are used to measure the exhaust gasses and inlet air temperature

2.2 Test procedure

Measured parameters included engine speed, engine power (calculated from the dynamometer reading), fuel consumption, inducted air mass flow rate, fuel line pressure, and cylinder pressure. The measurements were carried in the range from 1000 to 3000 rpm with 250 rpm increment. At each speed, the engine external load was adjusted to 0, 50, 100, 150, 200 and 250 N.m which corresponds to 0, 2.25, and 4.5, 6.75 and 9 bar brake mean effective pressure (BMEP).

The test procedure is required to fulfill the following main tasks in the prescribed order: first, pre-operational checks and preparations. Then, running the engine and sustaining the operating conditions as requested,(speed and load).Finally. Safety monitoring, e.g. overheating over-speed and overload.

3. Results and Discussions

3.1 In-cylinder and Fuel Line Pressures

In-cylinder pressure records investigation is the mainly efficient method to examine the engine combustion performance due to the direct effects of in-cylinder pressure history on the engine output power and combustion behavior characteristics. In this paper, in-cylinder pressure is recorded versus crank angle. Cycle to cycle variation was tested with the number of cycles. It was notice that the cycle

to cycle variation is constant for the number of cycles more than 30 cycles. Average pressure values for 42 successive cycles is calculated to evade the cycle to cycle variations and to report for measurement uncertainty.

In HCCI engines The combustion is divided into two subsequent processes namely; low-temperature process (cold flame) and high-temperature process with relatively small ignition delay period which strongly depends on the energy released during the low-temperature process [31].Ebrahimi and Desmet [22] introduced some fundamental combustion parameters of HCCI engine as shown in figure2.$HRRH_{max}$ and $HRRL_{max}$ are the maximum rates of heat release of high and low-temperature processes (reaction). In the first stage, the following parameters are defined. LTRA and LTRE are the low-temperature reaction appearance and end which are the points of intersection of the horizontal axis and the tangent line of the point where the gradient is maximum on the rising side and falling sides of the curve respectively. LTRD is the low-temperature reaction duration which is the duration between LTRA and LTRE. HTRA and HTRE are the high-temperature reaction appearance and end which are the points of intersection of the horizontal axis and the tangent line of the point where the gradient is maximum on the rising side and falling sides of the curve respectively. HTRD is the high-temperature reaction duration which is the duration between LTRA and LTRE. but for the second-stage combustion. The zone of negative temperature coefficient (ZNCT) is the period between FRBT and ARHT is named
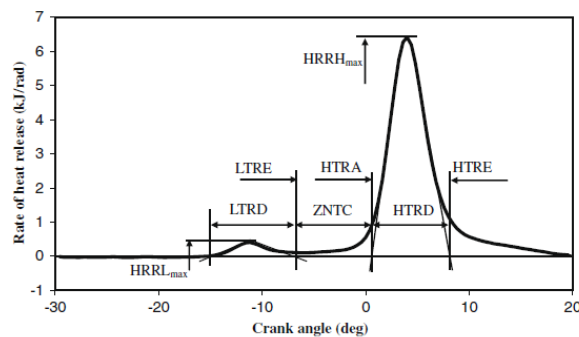
Figure 2. Definition of symbols and combustion parameters [22].

The apparent (net) heat release rate AHRR generally used in the literature is calculated by [32,33]

$$AHRR = \frac{dQ_{app}}{dt} = \frac{\gamma}{\gamma - 1} pdv + \frac{1}{\gamma - 1} vdp$$

Pressure-crank angle (P-φ) diagram provides information about combustion start, rate of pressure rise (pressure roughness), and maximum cylinder pressure.

The variation in in-cylinder pressure and apparent Heat Release rate are represented versus engine speed in figures 3 and 4.The speed changes from 1000 to 3000 rpm at a constant load of 200 N.m. It is noticed that there is more than one peak in P-φ history. This is a characteristic of multiple injection strategies of HCCI engines. The figures shows that the auto-ignition (during HCCI combustion) takes place in all cases. It is seen that heat is released in waves. These waves follow the injection pattern (pilot and main injections). The number of burning waves, however, is not the same in all cases, but changes with engine speed. It is directly obvious that as the engine speed increased the phasing of the main energy release shifts to later in the engine cycle. Also as the engine speed increases the magnitude of the low-temperature flame energy release becomes greater with fewer burning waves. The crank angle delay between the low temperature and the main flame energy release becomes longer for higher speeds. It is hypothesized that the HCCI auto ignition process is largely kinetically controlled, which is to say it is time-based [16]. The crank angle is directly proportional to the engine speed.Figure4shows that LTRD, ZNTC, and HTRD based on a crank angle are observed to increase

with increasing the engine speed. As a result, the angle-scale interval of chemical reactions increases. The engine speed has a remarkable influence on LTRD in spite of the other parameters.

Figures 5 and 6 dedicate the in-cylinder pressure variation recorded versus the crank angle for an engine speed of 3000 rpm and different loads of 50, 100, 150 and 200 N.m. The high-pressure rise line is shifted lower crank angle as the load increases (amount of injected fuel increases). As the mixture becomes richer (higher engine load), the start of combustion shifts towards earlier times (crank angle) due to the presence of a satisfactory amount of fuel at higher temperatures and pressure which leads to an earlier auto-ignition of charge. The maximum pressure is shown to increase as engine load increases.
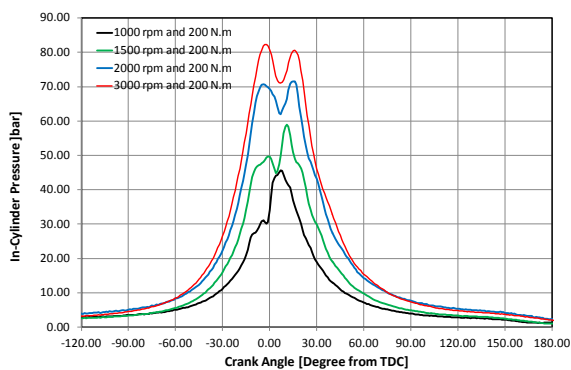
Figure 3. Cylinder pressure variation versus to crank angle for a constant load of 200 N.m and different engine speed.
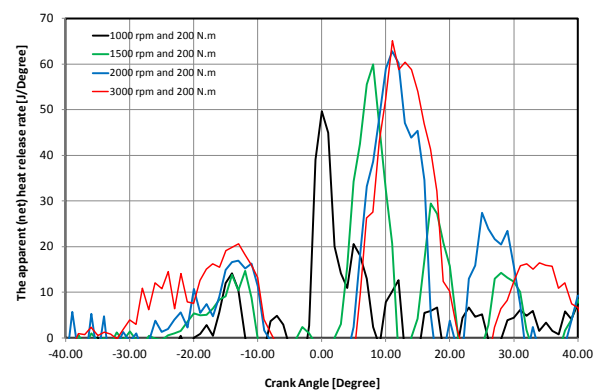
Figure4. Apparent Heat Release rate versus to crank angle for a constant load of 200 N.m and different engine speed**.**
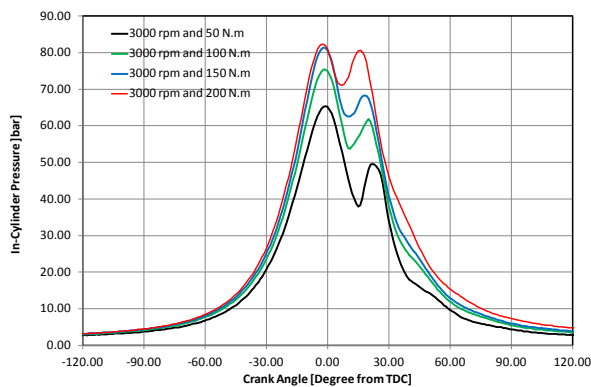
Figure 5. in-cylinder pressure variation versus crank angle for an engine speed of 3000 rpm and different loads.
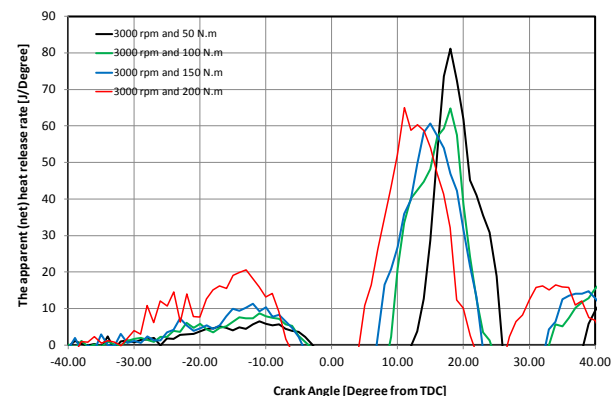
Figure6. Apparent Heat Release rate variation versus crank angle for an engine speed of 3000 rpm and different loads.

Figure 3 and figure 5 indicate that the crank angle interval at any in-cylinder pressure becomes larger as engine speed and load increases so for the same injected fuel the maximum pressure and so the maximum temperature may be decreased at high loads due to the distribution of high-pressure values on larger crank angle duration. This effect may be attributed to multiple injection strategies used in HCCI engines.

The measured fuel line pressure showed a repetitive pattern which is related to the pressure wave initiated at the beginning of each injection, it depends on the lengths of fuel pipes and a common rail in addition to the fuel bulks' modulus at each condition. The disturbances in the pressure distribution, due to injector and pump flow, propagate back and forth inside of the rail, reflecting off of the ends.

Initial pressure distribution in the rail superimposes onto the pressure distribution that is generated by the next injection [34].Figure 7shows the fuel line pressure variation versus crank angle for an engine speed of 3000 rpm and different loads of 50, 150 and 200 N.m. The average value of fuel line pressure increased from 1408 bar at 50 N.m brake load to 1584 bar at 150 N.m then increased to 1610 bar at 200 N.m which may be attributed to higher wave amplitude encountered due to the increase of the injector opening duration which promote the building up of pressure wave and retard the reverse of wave travel direction which helps in damping of the wave generated at the moment of injector opening.
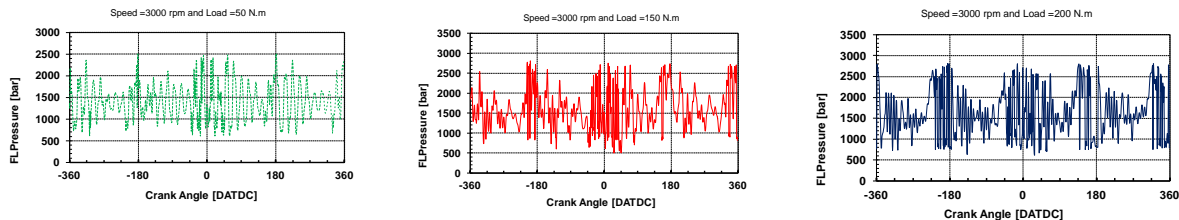
(a)   Engine load of 50N.m   (b)Engine load of 150N.m   (c)Engine load of 200N.m
Figure 7. Fuel Line pressure variation versus crank angle for an engine speed of 2000 rpm and different loads.
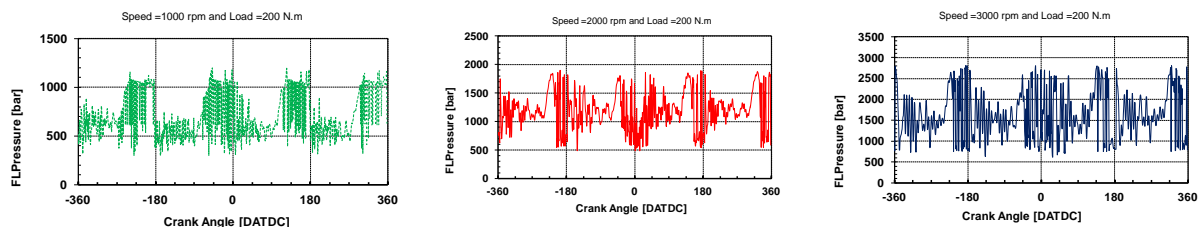
(a)   Engine load of 50N.m   (b)Engine load of 150N.m   (c)Engine load of 200N.m
Figure 8. Fuel line pressure variation versus crank angle for a constant load of 200 N.m and different engine speed.

Figure 8 shows the fuel line pressure variation versus crank angle for a constant load of 200 N.m and different engine speeds of 1000, 2000 and 3000 rpm. The average value is found to increase from 750bar at 1000 rpm to 1150 bar at 2000 rpm to 1610 bar at 3000 rpm. This is may be attributed to the higher flow rate of the high-pressure pump at higher speed and the higher wave amplitude encountered due to the increased number of injectors opening at a higher speed. However, the fuel line pressure needs more analysis in the crank angle domain and time domain which is the matter of future work. The effect of engine speed on pressure fluctuation is more dominant than that the effect of engine load. Alzahabi[34] concluded that fluctuation in the fuel line pressure promotes the fluctuation in fuel delivery. The pressure fluctuation is not enough to cause emissions problems at engine part loads but is enough to cause problems at full load.

3.2 Engine Performance
Figures (8(a) to 13a) show the speed characteristics of the turbocharged common rail diesel engine at different speeds from 1000 to 3000 rpm. Performance curves are presented at 6 fixed external loads, namely 0.0, 50, 100, 150, 200 and 250 N.m corresponding to 0, 2.25,4.5, 6.75, 9 and 11.25 bar BMEP in preference of brake torque. The results at each load are plotted against engine speed.
For a sake of preference, the speed characteristics of a turbocharged diesel engine with a conventional direct injection system are presented in figures (8b-13b). The technical specifications of the conventional engine are attached in appendix A. Performance curves are presented at 5 fixed external loads, namely 0.0, 70, 140, 210, 200 and 280 N.m corresponding to 0, 1.56, 3.11, 4.67 and 6.22   bar BMEP in preference of brake torque [35].

The engine power shown in figure 8(a) is a direct function of engine speed and brake mean effective pressure (BMEP). This is clear from the linear dependence on speed drawn at fixed BMEP. Comparing figure 8(a) and figure 8(b) on can find that the maximum presented power is 79.57 kW at 3000 rpm (Specific power of 28.8 kW/liter swept volume) for Common rail injection engine and 82.38 kW at 2800 rpm (Specific power of 14.5 kW/liter swept volume) for the conventional injection diesel engine which means that the two engines produce almost the same power at the same speed but at completely different BMEP which is 11.25 bar for common rail and 6.22 bar for the conventional engines so it is clear that the specific power of common rail engines is much greater than that for conventional injection engines.
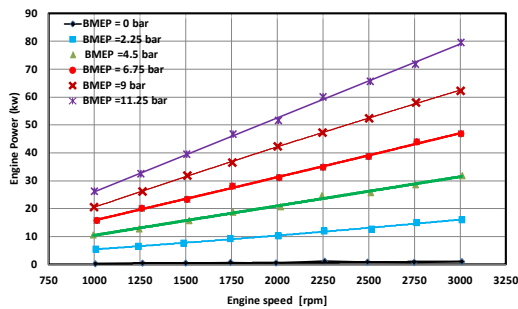
Figure 8(a). Engine power for diesel engine equipped with a common rail.
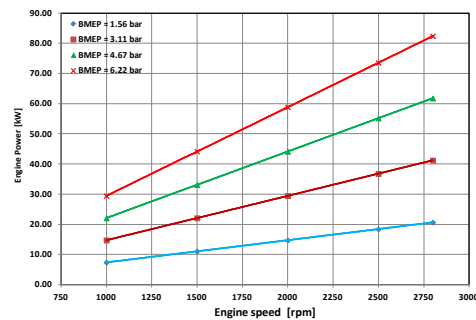
Figure 8b. Engine power for diesel engine equipped with a conventional injection system.

The equivalence ratio for the two engines is presented in figures 9(a) and 9(b). The mixture equivalence ratio increases with the brake mean effective pressure. This is due to the greater amount of fuel injected when higher loads are required. The effect of higher speed is attributed to better pump efficiency and fuel line expansion behavior. The figures reveal comparable results at the maximum load (BMEP). At lower external loads comparable results could be obtained at the same rations of $BMEP/BMEP_{max}$.

The brake specific fuel consumption (BSFC) presented in figure 10is shown to have an increasing trend with the decrease in engine speed due to the colder engine and bad charge mixing at low speeds. Then it is shown to increase again with the speed increase. This may be attributed to the higher friction losses at higher engine speed especially at part loads. The specific fuel consumption of the common rail injection engine (minimum value 210 gm/kW. hr at 2000 rpm and 11.25 bar BMEP) is much lower than that for the conventional engines (minimum value 292 gm/kW. hr at 2000 rpm and 6.22 bar BMEP). This because the displacement volume of the conventional engine is higher than that of the common rail injection engine and both working with the same fuel and equivalence ratios and the better utilization of fuel attained by high-pressure injection. The thermal efficiency is inversely proportional to the brake specific fuel consumption which is clear by comparisons of figures. 10 and 11.
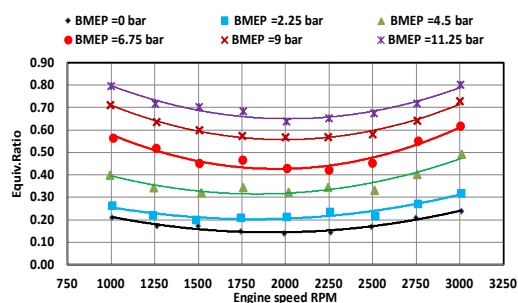
Figure 9(a). Equivalence ratio for diesel engine equipped with a common rail.
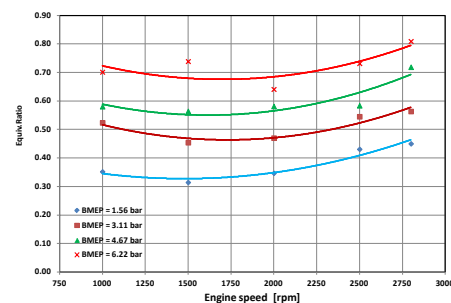
Figure 9(b). Equivalence ratio for diesel engine equipped with a conventional injection
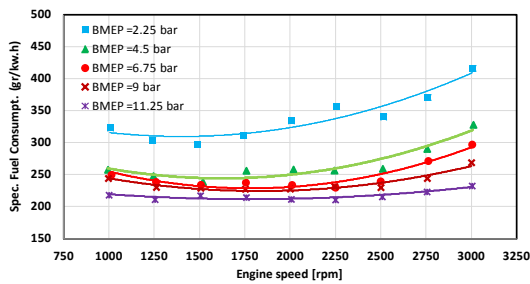
Figure10(a). BSFC for diesel engine equipped with a common rail injection system.
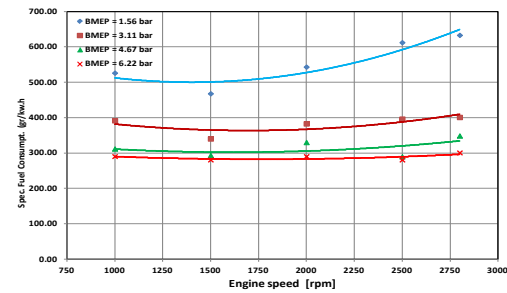
Figure 10(b). BSFC for diesel engine equipped with a common conventional injection system
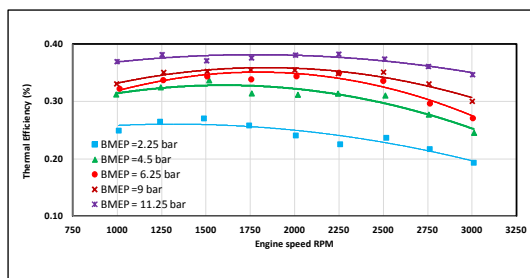
Figure 11(a). Thermal efficiency for diesel engine equipped with a common rail.
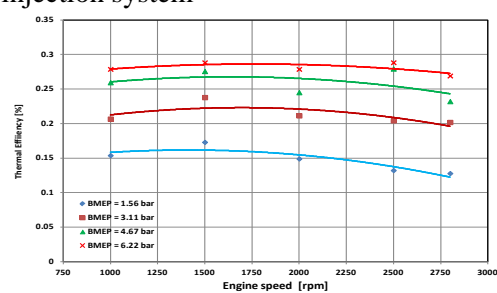
Figure 11(b). Thermal efficiency for diesel engine equipped with a conventional injection system.

Exhaust gas temperature shown in figure 12 is shown to increase with engine speed and load. The effect is explained by the less amount of heat transferred to cylinder walls as engine speed increases, and hence more heat is carried away with the exhaust. The effect of the increased load is a direct result of the more fuel injected and consequently more heat evolved during the combustion processes. The exhaust temperature of the common rail injection engine is much lower than that for the conventional engines. This may be attributed to the lean mixture that HCCI uses to lower the maximum combustion temperature resulting in reducing the engine exhaust temperature.

The volumetric efficiency calculated based on the air density achieved with turbocharging is shown in Figure 13. The volumetric efficiency of the common rail injection engine and conventional injection engine are almost similar except the engine speed at maximum volumetric efficiency which corresponds to the speed at which maximum torque occurs for both engines.
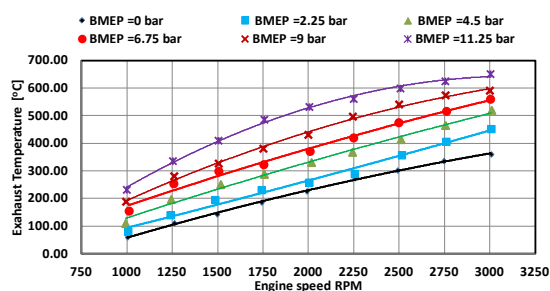
Figure 12(a). Exhaust temperature for diesel engine equipped with a common rail.
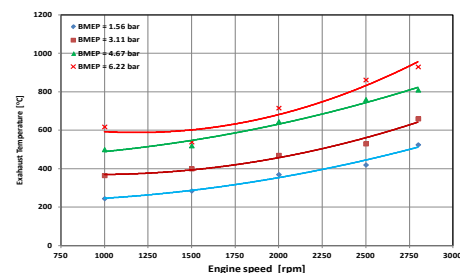
Figure 12(b). Exhaust temperature for diesel engine equipped with a conventional injection system.
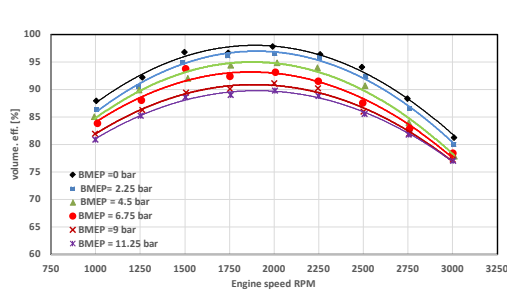
Figure 13(a). Volumetric efficiency for diesel engine equipped with a common rail injection system**.**
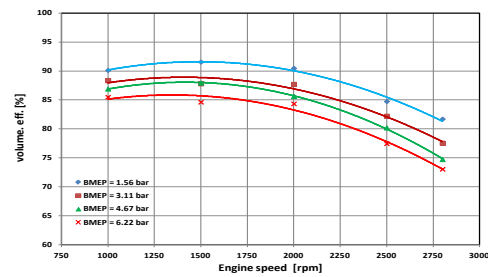
Figure 13(b). Volumetric efficiency for diesel engine equipped with a conventional injection system**.**

4. Conclusions

In the absence of studying the performance of HCCI engines at different loads, the objective of this work is to experimentally investigates the performance of an HCCI Diesel engine Common Rail Direct Injection (DI) fuel system. The engine performance is evaluated and presented at different loads and speeds.The analysis of in-cylinder pressure, heat release rate and fuel line pressure were performed to investigate the combustion behavior characteristics. The major conclusions from these investigations are listed below:

- The power density of the HCCI engine is much higher than of the conventional engine.
- The HCCI engine has higher thermal efficiency and lowers exhaust temperature than that for the conventional engine at all speed and loads
- The maximum in-cylinder pressure and temperature may be decreased at high loads due to the distribution of high-pressure values on larger crank angle duration. This effect may be attributed to multiple injection strategies used in HCCI engines. This may be advantageous in decreasing Nox or may give the chance to increase the engine compression ratio.
- LTRD, ZNTC, and HTRD based on the crank angle-scale increase with the increase of engine speed. So the chemical reaction intervals increase.
- As engine load increases (the mixture becomes richer), the start of combustion shifts towards BTDC side. Also as the engine speed increases the magnitude of the low-temperature flame energy release becomes greater with fewer burning waves. The crank angle delay between the low temperature and the main flame energy release becomes longer for higher speeds.
- The pressure wave amplitude generated in the high-pressure line due to the opening of the injector is shown to increase as engine speed and load increase. The effect of engine speed on pressure fluctuation is more dominant than that the effect of engine load. The fuel line pressure needs more analysis in crank angle domain and time domain which is the matter of future work

5. References

[1]   Zhao H 2007 *HCCI and CAI engines for the automotive* industry (Cambridge England: Wood head Publishing Limited).
[2]   Mathivanan K, Mallikarjuna J M and Ramesh A 2016 *Experimental Thermal and Fluid Science* 77 pp 337-346
[3]   Yoon, S H, Kim H J and Park S 2018 *Applied Thermal Engineering* **144** pp 1081-1090.
[4]   Han Z, Uludogan A, Hampson G and Reitz R 1996 *SAE* **960633.**
[5]   Khandal S, Banapurmath N,Gaitonde V and Hiremath S 2017 *Renewable and Sustainable Energy Reviews* **70** pp 369–384
[6]   Epping K, Aceves S, Bechtold R and Dec J 2002 *SAE Technical Paper* **2002-01-1923**.
[7]   Agarwal K, SinghA P and Maurya R K 2017 *Progress in Energy and Combustion Science*, **6**1 pp 1-56.

[8]   Han S, JaeheunKim J, and Bae C 2014 *Applied Energy* **119** pp 454–466
[9]   Wang X, Huang Z, Zhang W, Kuti O and Nishida K 2011 *Applied Energy* **88** pp1620–1628
[10]   Nishida K, Zhu J, Leng X and He Z 2017 *International J of Engine Research* **18**(1-2) pp 51–65.
[11]   Nathan S, Mallikarjuna S and Ramesh A 2009 *SAE* **2009-26-028** .
[12]   Najt P and Foster D 1983 SAE **830264**.
[13]   Kong S and Reitz R 2002 *J. Eng. Gas Turb. Power ASME* **124** pp 702–7.
[14]   Kong S, Marriott C, Reitz R and Christensen M 2001 *SAE* **2001-01-1026**.
[15]   Iida M, Aroonsrisopon T, Hayashi M, Foster D and Martin J 2001 *SAE* **2001-01-1880/4278**
[16]   Aroonsrisopon T, Foster DE, Morikawa K and Lida M 2002 *SAE* **2002-01-1924; 2002**.
[17]   Iida M, Hayashi M, Foster D and Martin J 2003 *J. Eng. Gas Turb. Power ASME* **125** pp427–78.
[18]   Szybist J and Bunting B 2005 *SAE* **2005-01-3723**.
[19]   Garcia M, Aguilar F and Lencero T 2009 *Energy* **34** pp 159–71.
[20]   Genzale C, Kong S and Reitz R 2008 *J. Eng. Gas Turb. Power ASME* **130** p 8.
[21]   Maurya R and Agarwal A 2009 *SAE* **2009-01-1345**.
[22]   Ebrahimi R and Bernard Desmet B 2010 *Fuel* **89** pp 2149–2156
[23]   Hadia F, Wadhah S, Ammar H and Ahmed O 2017 *Case studies in thermal engineering* **10** pp 262-271.
[24]   Alper Calam A, Solmaz H, Icingur Y and Yilmaz E 2018 *Energy* **168** pp 1208-1216
[25]   Shenawy E,   Elkelawy M, Bastawissi H A, Panchal H and Shams M 2019 *Fuel* **249** pp 277–285
[26]   Ganesh D and Nagarajan G 2010 *Energy* **35(1)** pp148–57.
[27]   Yu S, Li L and Zheng M 2019 *Fuel* **242** pp 243–54.
[28]   Liu H, et al 2018 *Fuel* 231 pp 26–36.
[29]   Lu X, Han D and Huang Z 2011 *Prog. Energy Combust Sci*. **37(6)** pp741–83.
[30]   An Y et al 2018 *Energy* **158** pp181–91.
[31]   Tanaka S, Ayala F, Keck J and Heywood J 2003 *Combustion and Flame* **132** pp 219–239
[32]   Asad U, Zheng M 2008 *International Journal of Thermal Sciences* **47** pp 1688–1700
[33]   Fathi M, Saray R K, Checkel M D 2010 *Fuel* **89** pp 2323–2330
[34]   Alzahabi B and Schulz K 2008 *Int. Jnl. of Multiphysics* **2** Number 3
[35]   Elmaihy A 1997 MSc. thesis, Military Technical Collage.

Appendix A: **Engine Technical Data**

Make and Model	Mercedes 352 seriesNatural aspiratedDiesel engine
Compression ratio	17: 1
No. of Strokes	4
No. of cylinder	6
Arranging	In-line
Cooling	Water
Bore	97 mm
Stroke	128 mm
Combustion chamber	Open type, Direct Injection
Camshaft	Sided
Speed range	800-2800 rpm
Maximum power	120 HP at 2800 rpm
Maximum torque	28 kp.m at 1600 rpm
Static injection	23 CA BTDC
Firing order	1 5 3 6 2 4 1
Min.compression pressure	20 bar at 150-200 rpm
Injector opening pressure	200 bar